Journal of Photochemistry and Photobiology A: Chemistry 251 (2013) 154–159

Contents lists available at SciVerse ScienceDirect

Journal of Photochemistry and Photobiology A: Chemistry

journal homepage: www.elsevier.com/locate/jphotochem

Photoluminescent PMMA polymer films doped with Eu^{3+}-β-diketonate crown ether complex

Edison B. Gibelli[a], Jiang Kai[b,c], Ercules E.S. Teotonio[d], Oscar L. Malta[e], Maria C.F.C. Felinto[a], Hermi F. Brito[b,*]

[a] Centro de Química e Meio Ambiente, Instituto de Pesquisas Energéticas e Nucleares, 2242 Av. Prof. Lineu Prestes, 05508-000, São Paulo, SP, Brazil
[b] Instituto de Química, Universidade de São Paulo, 748 Av. Prof. Lineu Prestes, 05508-000, São Paulo, SP, Brazil
[c] Departamento de Química, Pontifícia Universidade Católica de Rio de Janeiro, Gávea, 22451-900, Rio de Janeiro, RJ, Brazil
[d] Departamento de Química, Universidade Federal da Paraíba, Cidade Universitária, 58051-970, João Pessoa, PB, Brazil
[e] Departamento de Química Fundamental – CCEN, Universidade Federal da Pernambuco, Cidade Universitária, 50740-540, Recife, PE, Brazil

ARTICLE INFO

Article history:
Received 26 July 2012
Received in revised form 8 October 2012
Accepted 23 October 2012
Available online 5 November 2012

Keywords:
Europium complexes
Crown ethers
PMMA
Luminescent film

ABSTRACT

In this work it is reported the photoluminescence sensitization effect of the bis(dibenzo-18-crown-6)diaquatris(thenoyltrifluoroacetonate)europium(III) compound, $[Eu(tta)_3(DB18C6)_2(H_2O)_2]$, doped into a blend of poly(methylmethacrylate) (PMMA) and polyethylene glycol (PEG) in film form. The TGA results indicate that the Eu^{3+}-complex precursor is immobilized in the polymer matrix by the interaction between the Eu^{3+} complex and the oxygen atoms of the PMMA polymer. The thermal behavior of these luminescent systems is similar to that of the undoped polymer. The emission spectra of the Eu^{3+}-complex in the PMMA/PEG blends recorded at room temperature exhibit the characteristic bands arising from the $^5D_0 \rightarrow {}^7F_J$ ($J = 0$–4) intraconfigurational transitions. The emission quantum efficiency of the Eu^{3+} ion doped films increased significantly, indicating an effective interaction between the Eu^{3+}-complex and the polymer matrix, and both the substitution of water molecules in the first coordination sphere and an efficient luminescence co-sensitization of the Eu^{3+} luminescent centers.

1. Introduction

Rare earth (RE^{3+}) β-diketonate complexes have been extensively investigated in recent years as promising candidates for luminescent materials [1–7]. These RE^{3+} compounds present characteristic narrow emission bands in the UV–vis region with excitation and emission monitored in different spectral regions, and antenna effect that enhances the emission quantum yield. As a result, these complexes have found wide applications as optical markers, photoluminescent sensors, electroluminescent devices and multicolor displays [8–10].

Polymers doped with RE^{3+}-complexes have attracted considerable interest because they preserve the luminescence properties of the complexes while they can be processed from solution and are mechanically flexible [10,11]. For instance, the stable transparent mixtures could be easily spin-coated and thermally converted to uniform films. Therefore, a polymeric system incorporated with rare earth complexes is expected to be integrated in functional devices, such as polymer fiber laser, waveguide amplifiers and compact lasers that constitute a major part of the ever-growing field of photonics [12].

The poly(methylmethacrylate) (PMMA) possesses many desirable properties, such as high light transmittance, chemical resistance, colorless, resistance to weathering corrosion, good insulating properties, low optical absorption, refractive index tailorability with molecular weight, simple synthesis, and low cost [12]. These characteristics make it suitable as a host material for RE^{3+} ions and organic dye doping. The non-toxicity of PMMA resulted in amplified utilization in dentures, medicine dispensers, food-handling equipments, throat lamps and lenses [13]. Moreover, PMMA embedding inorganic or organically modified inorganic particles has been cast into films to yield enhanced functional properties such as electrical conductivity [14], photoconductivity [15], photo-induced charge-transfer, nonlinear optical properties, photoluminescence [16–24], mechanical [25–30] and magnetic properties [30,31].

In the present work, a series of the trivalent europium chelate $[Eu(tta)_3(DB18C6)_2(H_2O)_2]$ (DB18C6: dibenzo-18-crown-6) doped PMMA films in the absence or presence of Polyethyleneglycol PEG300 and 400 was prepared and characterized. It was also studied the influence of the chemical structure of the ligand and PEGs on the luminescence properties of the Eu^{3+}-complex doped PMMA/PEGs. The experimental 4f–4f intensity parameters have been calculated and discussed.

* Corresponding author. Tel.: +55 11 30913708; fax: +55 11 38155579.
E-mail address: hefbrito@iq.usp.br (H.F. Brito).

1010-6030/$ – see front matter © 2012 Elsevier B.V. All rights reserved.
http://dx.doi.org/10.1016/j.jphotochem.2012.10.015

2. Experimental

All materials oxides, ligands, acid and base were purchased (Sigma–Aldrich, Merck, Across) and used without further purification. PMMA was supplied in powder form by Aldrich, presenting an average molecular weight (Mw) of approximately 350,000 g mol^{-1}, with PMMA accounting for 99.9% of the dry material.

2.1. Synthesis of the $[Eu(tta)_3(H_2O)_2]$ complex

Crystals of the precursor $[Eu(tta)_3(H_2O)_2]$ complex were synthesized as described in the literature [6] where 2-thenoyltrifluoroacetone (1.33 g; 6 mmol) was dissolved in 30 mL of ethanol. NaOH (1 mol L^{-1}; 6 mL) and a solution of $EuCl_3{\cdot}6H_2O$ (0.73 g; 2 mmol) in 10 mL of distillated water were successively added to the tta solution. Water (200 mL) was added and the mixture was heated to 60 °C for a few minutes. The complex precipitated during cooling to room temperature. The precipitate was filtered then washed with water and dried under reduced pressure with a yield of 90%.

2.2. Synthesis of the $[Eu(tta)_3(DB18C6)_2(H_2O)_2]$ compound

The precursor complex (1 g, 1.17 mmol) and crown ether ligand (0.8436 g, 2.34 mmol) were dissolved separately in ethanol and mixed under stirring until the formation of a paled yellow precipitate. The crystalline solids were washed with ethanol, dried under reduce pressure and stored in a vacuum desiccator [5].

2.3. Preparation of the films

The PMMA powder (0.3 g) was dissolved in 100 mL of acetone followed by addition of 1% (w/w) of the Eu^{3+} complex (0.003 g, 0.0019 mmol) also dissolved in acetone. The resulting solution was heated at 60 °C for 30 min then the polymer film (denoted as P/Eu film) was obtained after the evaporation of excess solvent at 60 °C. The same procedure was used for the films of the PMMA/PEG blend, differing only by the addition of 1% (w/w) of PEG300 and 400 in the final step, which are denoted as P/Eu/G300 and P/Eu/G400.

2.4. Characterization techniques

Carbon and hydrogen contents were determined by usual microanalytical procedures using an elemental analyzer model CHN 2400 (Perkin-Elmer). The Eu^{3+} content was estimated by spectrophotometer analyses with Alizarin Red S as chromophore agent in methanol solution.

Thermogravimetric analysis (TGA) was achieved with a TG/SDTA 822 thermobalance (Mettler-Toledo), using sapphire crucibles containing around 5 mg of the sample, under dynamic nitrogen atmosphere with stream of (50 mL min^{-1}), at a heating rate of 10 °C min^{-1}.

The infrared absorption spectra of the samples were acquired at room temperature using a Thermo Nicolet model 6700 Continuum FTIR spectrophotometer. The spectra were collected in the 4000–400 cm^{-1} range by averaging at least 80 scans at a resolution of 4 cm^{-1}. Prior to recording the spectra the films were kept under reduced pressure at room temperature for several days in order to reduce the levels of adsorbed water molecules.

Scanning electronic micrographies (SEM) were obtained in a microscope Philips XR-30 by means of a sputtering technique using gold as recovering material.

The excitation and emission spectra of the powdered and film samples were recorded in a SPEX Fluorolog-2 spectrofluorometer, model FL212 system, 450 W Xenon lamp as excitation source and double grating 0.22 m SPEX 1680 monochromators. All spectra were recorded using a detector mode correction. The luminescence decay curves of the emitting levels were measured using a phosphorimeter SPEX 1934D accessory coupled to the spectrofluorometer.

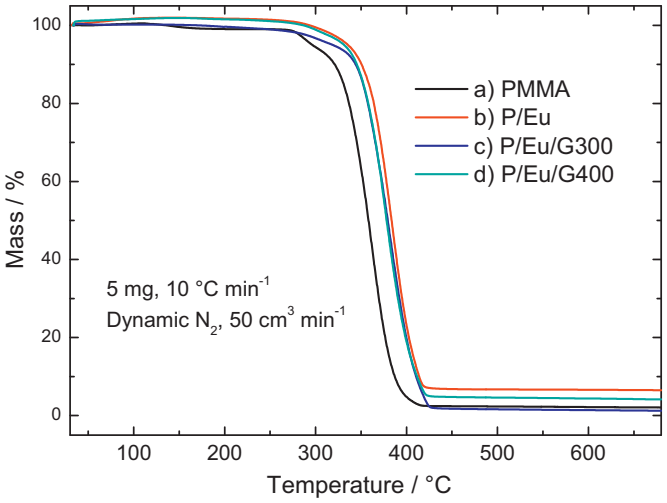

Fig. 1. TGA curves of (a) undoped PMMA, (b) P/Eu, (c) P/Eu/G300 and (d) P/Eu/G400 blend films. All these data were recorded under an inert atmosphere of dynamic N_2.

3. Results and discussion

The C and H contents in the Eu^{3+} complex determined by the elemental analytical methods agree with the formula $[Eu(tta)_3(DB18C6)_2(H_2O)_2]$; calculated for $Eu_1O_{20}C_{64}H_{48}F_9S_3$ was: C, 48.80%; H, 4.80% and found: C, 48.36%; H, 4.85%.

Fig. 1 shows the thermogravimetric curves of the samples in film form of undoped PMMA polymer and PMMA doped with the Eu^{3+} complex at a ratio of 1% (w/w) and PMMA and PEG blends recorded under an inert N_2 atmosphere. As can be seen, the TGA curves (Fig. 1) recorded in the temperature interval from 25 to 200 °C exhibited no mass loss event. This fact reveals that the water molecules coordinated to the Eu^{3+} ion of the hydrate precursor complex are absent after the doping reaction. Therefore, the $[Eu(tta)_3(DB18C6)_2(H_2O)_2]$ complex is embedded in the PMMA polymer matrix by the chemical interaction between the Eu^{3+} complex and the oxygen atoms of the PMMA polymer or PEG where the two water molecules are replaced. These results agree with other polymer systems previously analyzed [11].

It is shown in Fig. 1a that the undoped PMMA polymer film decomposes in a one-step event and its degradation starts at 281 °C. Similarly, the PMMA polymer doped with the Eu^{3+} complex also presented a curve of decomposition under an inert atmosphere with one single decomposition event only. As indicated in Fig. 1b–d the doped PMMA films exhibit decreasing onset temperatures of decomposition (T-onset) of 238, 255 and 231 °C for the P/Eu, P/Eu/G300 and P/Eu/G400 blends, respectively. The maximum displacement of T-onset was 50 °C for the P/Eu/G400 blend in comparison to that of the undoped polymer film.

The IR absorption spectrum of doped PMMA film (Fig. 2a) displays a very strong peak at around 1731 cm^{-1} assigned to the ν(C=O) stretching band of non-conjugated ester (free carbonyl group). Another series of peaks was identified at 1484, 1449 and 1436 cm^{-1} that is characteristic of the ν(O—CH_3) ester group. The bands around 1065 and 1270 cm^{-1} are stretching vibration modes of the C—O—C group. A strong broad band is observed at about 2995 cm^{-1} due to the stretching vibration modes of CH_3 and CH_2, indicating a high hydrogen content in the carbon backbone of PMMA. Besides, the absorptions at about 1450, 1385 and 1365 cm^{-1}

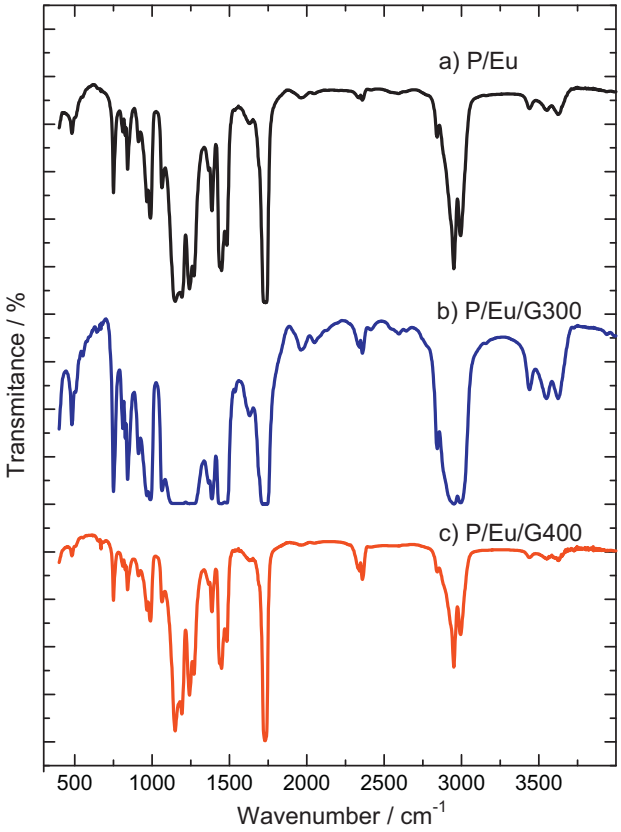

Fig. 2. IR absorption spectra directly registered in their film form of (a) P/Eu, (b) P/Eu/G300 and (c) P/Eu/G400 blends.

are attributed to in-phase and out-phase bending vibrations of CH_3. The weak absorption at 1191 and 1150 cm^{-1} is due to the in-plane C—H angle deformation. The IR spectra also show two very weak bands at 1635 and 1537 cm^{-1} attributed to νs(C=O) and νas(C=O) vibrational modes of the tta ligand that are in accordance with the tta group acting as a chelate ligand.

The main band to be observed in the IR spectra of the crown ether is the δC—O—C. In the present work, after the formation of the compound this characteristic band of asymmetrical axial deformation shifted to smaller frequencies around 1130 cm^{-1}, indicating the coordination of the crown ether to the Eu^{3+} ion.

The surface morphology was investigated by Scanning Electronic Microscopy (SEM) (Fig. 3a–f). In Fig. 3a it is observed the homogeneous crystallinity of the $[Eu(tta)_3(DB18C6)_2(H_2O)_2]$ complex precursor. When the PMMA was co-doped with the complex and PEG300, the resulting films showed a uniform porous structure (Fig. 3b and c). However, it can be observed from Fig. 3d–f that P/Eu/G400 displays a lace-like morphology. No significant phase separation is observed within the obtained blend polymer films doped with the Eu^{3+}-complex, indicating that the framework on the surface is homogeneous. This is possibly due to the preparation technique, through which all the compositions are mixed at a molecular level, indicating the occurrence of interaction between the Eu^{3+} complex and polymer matrix [31–33].

On the other hand, the doped films blended with PEG 300 and PEG 400 display different morphologies. Figs. 3e and f, at a higher magnification scale, present the formation of mesoporous sphere-shape particles linked to the lace fiber network. This result is owing to the different polymeric chain structures between the PEG 300 and PEG 400 that can affect the microstructure and the interaction between the polymer matrix and the precursor Eu^{3+}-complex.

3.1. Photoluminescence properties

The polymer films and doped blends are homogeneous crystal clear thin plastic films that display strong monochromatic red emission color under the irradiation with an ultraviolet lamp (366 nm). The photoluminescence sensitization process of the Eu^{3+} ion can be explained by the following steps: (i) energy of exciting UV light is absorbed by the ligands; (ii) the excited singlet state decays to the lowest triplet state of ligands; (iii) the energy is transferred from the triplet state of the ligands to the emitting $^5D_1$ and $^5D_0$ levels of the Eu^{3+} ion; (iv) the excited Eu^{3+} ion decays radiatively to the ^7F_J ground state in the visible region.

In Fig. 4 it is presented the excitation spectra of the $[Eu(tta)_3(DB18C6)_2(H_2O)_2]$ complex, P/Eu, P/Eu/G300 and P/Eu/G400registered at room temperature by monitoring the luminescence intensity of the $^5D_0 \rightarrow {}^7F_2$ transition at 614 nm. It is observed that in the spectral region from 250 to 420 nm, the polymeric doped films and blends exhibit two intense broad excitation bands centered at 389 and 309 nm, which can be attributed to transitions from the S_0 ground state to the S_1 excited state of the organic moiety. Furthermore, the typical intraconfigurational transitions of the trivalent europium ion exhibit very low intensity in these excitation spectra, corroborating with an efficient energy transfer from the organic moiety to the metal ion. These optical data suggest that the polymer matrices act as luminescent co-sensitizers and the organic ligands are efficient sensitizers for the Eu^{3+} ions.

Fig. 5 displays the emission spectra of the P/Eu, P/Eu/G300 and P/Eu/G400blends recorded at room temperature under excitation at 394 nm in the spectral range of 450 to 720 nm. These spectroscopic data present the typical emission narrow bands assigned to the characteristic $^5D_0 \rightarrow {}^7F_J$ transitions (J = 0–4) of the Eu^{3+} ion. The transition that shows the highest intensity is the hypersensitive $^5D_0 \rightarrow {}^7F_2$ transition around 614 nm. In addition, the presence of only one sharp peak of the non-degenerate $^5D_0 \rightarrow {}^7F_0$ transition at around 580 nm indicates a chemical environment around the Eu^{3+} ion of symmetry C_s, C_n or C_{nv}. The absence of the polymer broad emission band in the doped film in the range of 450–550 nm shows the high efficiency of the intramolecular energy transfer process via the polymer matrix to the Eu^{3+} ion, corroborating the interpretation in which the polymer matrix acts as an efficient co-sensitizer of the Eu^{3+} photoluminescence.

The luminescence decay curves of the doped films were obtained by monitoring the emission at the $^5D_0 \rightarrow {}^7F_2$ transition (614 nm) under excitation at the $^7F_0 \rightarrow {}^5L_6$ transition (394 nm). The decay curves were adjusted with a first-order exponential decay function and the lifetime values (τ) of the $^5D_0$ emitting level were determined (Table 1). All τ values of the doped polymer systems are higher than that of the hydrated Eu^{3+} precursor complex due to the substitution of water molecules in the first coordination sphere and, therefore, the decrease of non-radiative losses from the $^5D_0$ level.

Fig. 5 also exhibits the inhomogeneous line broadening effect for the $^5D_0 \rightarrow {}^7F_J$ transitions (J = 0–4) of the P/Eu, P/Eu/G300 and P/Eu/G400 luminescent materials in comparison to the narrow emission bands of the $[Eu(tta)_3(DB18C6)_2(H_2O)_2]$ precursor (Fig. 5 inset). This is a consequence of a distribution of slightly different sites of symmetry occupied by the rare earth ion upon incorporation into the PMMA polymer.

The emission quantum efficiency (η) of the $^5D_0$ excited state of the europium ion is determined by the following expression [2,34–36]:

$$\eta = \frac{A_{rad}}{A_{rad} + A_{nrad}} \quad (1)$$

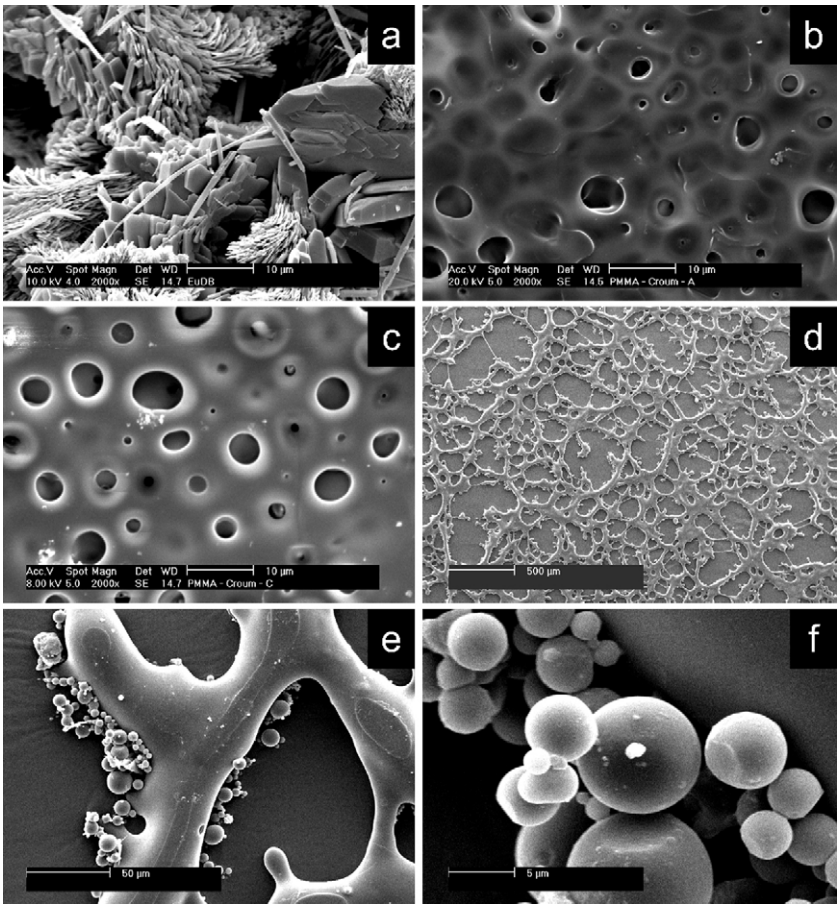

Fig. 3. SEM images of (a) $[Eu(tta)_3(DB18C6)_2(H_2O)_2]$ complex, (b) P/Eu, (c) P/Eu/G300, (d) P/Eu/G400 [500 μm], (e) P/Eu/G400 [50 μm] and (f) P/Eu/G400 [5 μm] blend films.

where A_{rad} and A_{nrad} are radiative and nonradiative transition rates, respectively. The denominator in Eq. (1) may be experimentally determined by adjusting the luminescence decay data to an exponential curve, and using the expression: $\tau = 1/(A_{rad} + A_{nrad})$, where τ is the lifetime of the emitting $^5D_0$ level.

The experimental radiative rates, A_{rad}, were determined by summing over the radiative rates A_{0J} for each $^5D_0 \rightarrow {}^7F_J$ transition, $A_{rad} = \Sigma A_{0J}$. The individual coefficients of spontaneous emission, A_{0J}, were determined by taking the $^5D_0 \rightarrow {}^7F_1$ magnetic dipole transition as internal reference [34]:

$$A_{0J} = A_{01}\left(\frac{I_{0J}}{I_{01}}\right)\left(\frac{V_{01}}{V_{0J}}\right) \quad (2)$$

where ν_{01} and ν_{0J} are the barycentres of the $^5D_0 \rightarrow {}^7F_1$ and $^5D_0 \rightarrow {}^7F_J$ transitions, respectively. I_{01} and I_{0J} represent the integrated intensity assigned to the $^5D_0 \rightarrow {}^7F_1$ and $^5D_0 \rightarrow {}^7F_J$ transitions, respectively.

These spontaneous emission coefficients A_{0J} were also used to determine the experimental intensity parameters (Ω_2 and Ω_4) according to the following equation:

$$A_{0J'} = \frac{e^2\omega^3}{3\hbar c^3(2J+1)}\chi\sum_{\lambda}\Omega_\lambda\left\langle {}^5D_{0'}||U^{(\lambda)}||{}^7F_J\right\rangle^2 \quad (3)$$

where ω is the angular frequency of the transition, e is the electronic charge, $\hbar$ is Planck's constant over 2π, c is the velocity of light and χ is the Lorentz local field correction that is given by $n(n^2+2)^2/9$ with the refraction index $n = 1.5$. The $\left\langle {}^5D_{0'}||U^{(\lambda)}||{}^7F_J\right\rangle^2$ values are the square reduced matrix elements whose values are 0.0032 and 0.0023 for $J = 2$ and 4, respectively. The Ω_6 intensity parameter was not included in this study since the $^5D_0 \rightarrow {}^7F_6$ transition was not observed.

All the emission quantum efficiency values of the P/Eu/G400, P/Eu/G300 and P/Eu doped polymer films are higher than that of the precursor $[Eu(tta)_3(DB18C6)_2(H_2O)_2]$ complex (Table 1). These

Table 1
Experimental intensity parameters (Ω_λ), emission quantum efficiencies (η), lifetimes (τ), radiative (A_{rad}) and non-radiative (A_{nrad}) emission coefficient rates for the $[Eu(tta)_3(DB18C6)_2(H_2O)_2]$ complex, P/Eu, P/Eu/G300 and P/Eu/G400 blend films, based on the emission spectra recorded at room temperature.

Sample	$\Omega_2 \times 10^{-20}$ cm^2	$\Omega_4 \times 10^{-20}$ cm^2	A_{rad} s^{-1}	A_{nrad} s^{-1}	τ (ms)	η (%)
Eu-complex[a]	31.0	11.6	1155	3345	0.222	26
P/Eu	32.2	7.7	1133	1571	0.370	42
P/Eu/G300	31.1	8.9	1122	1444	0.390	44
P/Eu/G400	48.1	12.8	1688	1217	0.344	58

[a] Ref. [5].

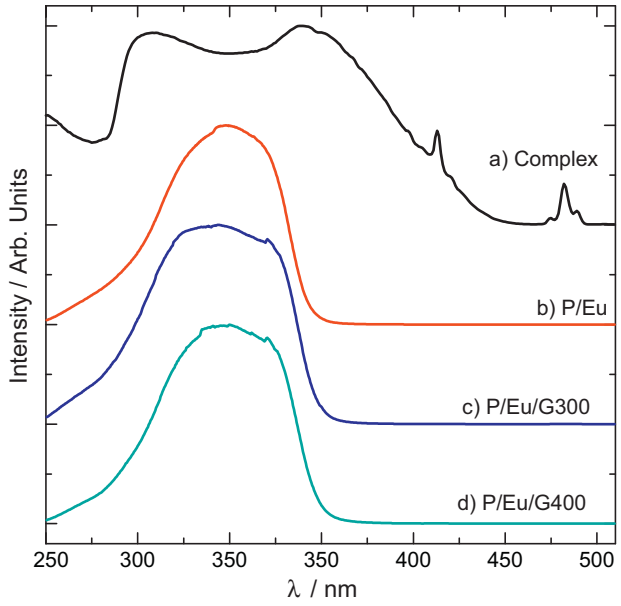

Fig. 4. Excitation spectra of (a) $[Eu(tta)_3(DB18C6)_2(H_2O)_2]$ complex, (b) P/Eu, (c) P/Eu/G300 and (d) P/Eu/G400 blend films registered at room temperature with emission monitored at 614 nm.

results confirm that the polymeric matrix is actually efficient in substituting the water molecules in the first coordination sphere.

The P/Eu/G400 film presents emission bands of higher intensity as compared with the other doped systems, as shown in Fig. 6. In addition, the PEG400 co-doped film also presented the highest value of emission quantum efficiency $\eta = 58\%$ (Table 1). On the other hand, the smallest value of $\eta = 42\%$ was observed for the P/Eu film, owing to its highest value of the non-radiative contribution ($A_{nrad} = 1571\ s^{-1}$). The experimental intensity parameters (Ω_2 and Ω_4) for the doped polymer films and precursor $[Eu(tta)_3(DB18C6)_2(H_2O)_2]$ complex are presented in Table 1.

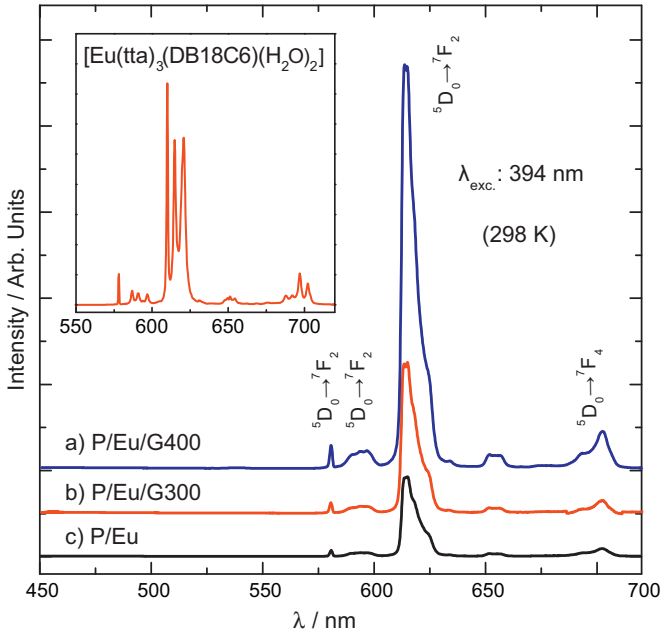

Fig. 5. Room temperature emission spectra of luminescent materials (a) P/Eu/G400, (b) P/Eu/G300 and (c) P/Eu, blend films, under excitation at 394 nm at room temperature. The inset figure shows the emission spectra of $[Eu(tta)_3(DB18C6)_2(H_2O)_2]$ complex.

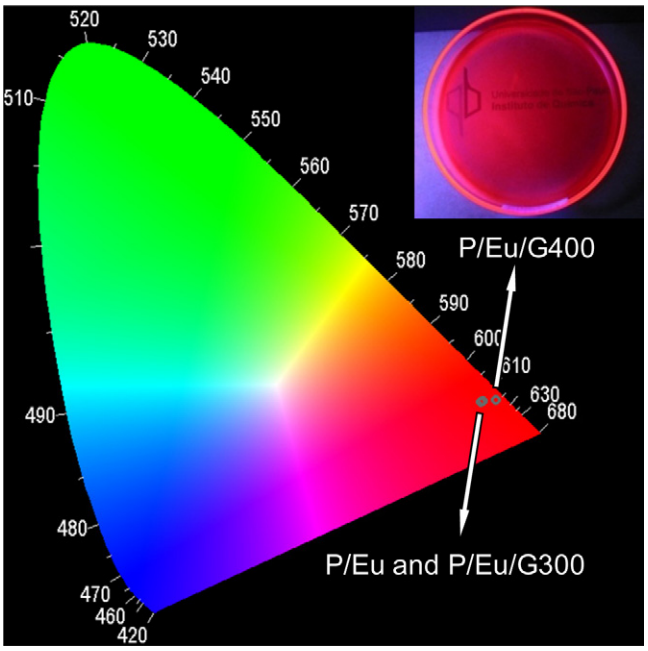

Fig. 6. CIE chromaticity diagram showing the *x*,*y* emission color coordinates of P/Eu, P/Eu/G300 and P/Eu/G400 blend films excited at 350 nm. The inset figure is photograph of P/Eu/G400 film taken with a digital camera displaying red emission under UV irradiation at 366 nm. (For interpretation of the references to color in this figure legend, the reader is referred to the web version of the article.)

The considerably high values of these parameters are consistent not only with a very low symmetry of the site occupied by the Eu^{3+} ion but also with large values of the ligating atom polarizabilities entering in the dynamic coupling mechanism of 4f–4f intensities, particularly in the P/Eu/G400 system.

The CIE chromaticity coordinates generated from the emission spectra of all systems (Fig. 6) with the europium complex are $x = 0.65$ and $y = 0.31$, indicating the red color monochromatic character [37].

4. Conclusion

The PMMA polymer co-doped with the complex $[Eu(tta)_3(DB18C6)_2(H_2O)_2]$ and PEG were prepared and characterized. The thermal behavior of PMMA polymer films doped with Eu^{3+}-complex and undoped PMMA film is similar. IR data indicate that the Eu^{3+} complex is anchored in the PMMA polymeric network by the coordination of the carbonyl oxygen atoms of the host polymer matrix toward the Eu^{3+} ions substituting water molecules in the first coordination sphere. SEM images showed that the films obtained are homogeneous and preserve the polymer aspects. The absence of the broad emission band of the polymer in the doped system indicated that intramolecular energy transfer via the polymer matrix to the Eu^{3+} ion is highly efficient, suggesting that the polymer matrix acts as a photoluminescence co-sensitizer. In addition, the higher values of emission quantum efficiency of the emitting $^5D_0$ level for the doped polymer films corroborate with the substitution of water molecules by the polymer carbonyl groups. The $[Eu(tta)_3(DB18C6)_2(H_2O)_2]$ doped PMMA/PEG systems, therefore, may act as efficient light conversion molecular devices.

Acknowledgements

The authors thank the Brazilian Agencies: CNPq, FAPESP, inct-INAMI and NANOBIOTEC-Brasil for financial support.

References

[1] K. Binnemans, Rare-earth beta-diketonates, in: K.A. Gschneidner Jr., J.-C.G. Bünzli, V.K. Pecharsky (Eds.), Handbook on the Physics and Chemistry of Rare Earths, Elsevier, Amsterdam, 2004, pp. 107–272.

[2] J.-C.G. Bünzli, Lanthanide luminescence for biomedical analyses and imaging, Chemical Reviews 110 (2010) 2729–2755.

[3] H.F. Brito, O.L. Malta, M.C.F.C. Felinto, E.E.S. Teotonio, Luminescence phenomena involving metal enolates, in: J. Zabicky (Ed.), Patai Series: The Chemistry of Metal Enolates, John Wiley & Sons Ltd, Chichester, England, 2009, pp. 131–184.

[4] S.V. Eliseeva, J.-C.G. Bünzli, Lanthanide luminescence for functional materials and bio-sciences, Chemical Society Reviews 39 (2010) 189–227.

[5] M.C.F.C. Felinto, C.S. Tomiyama, H.F. Brito, E.E.S. Teotonio, O.L. Malta, Synthesis and luminescent properties of supramolecules of b-diketonate of Eu(III) and crown ethers as ligands, Journal of Solid State Chemistry 171 (2003) 189–194.

[6] H.F. Brito, O.L. Malta, L.R. Souza, J.F.S. Menezes, C.A.A. Carvalho, Luminescence of the films of europium(III) with thenoyltrifluoroacetonate and macrocyclics, Journal of Non-Crystalline Solids 247 (1999) 129–133.

[7] K. Sheng, B. Yan, Coordination bonding assembly and photophysical properties of Europium organic/inorganic/polymeric hybrid materials, Journal of Photochemistry and Photobiology A: Chemistry 206 (2009) 140–147.

[8] X. Ouyang, R. Yu, J. Jin, J. Li, R. Yang, W. Tan, J. Yuan, New strategy for label-free and time-resolved luminescent assay of protein: conjugate Eu^{3+} complex and aptamer-wrapped carbon nanotubes, Analytical Chemistry 83 (2011) 782–789.

[9] A.K. Singh, S.K. Singh, H. Mishra, R. Prakash, S.B. Rai, Structural, thermal, and fluorescence properties of $Eu(DBM)_3Phen_x$ complex doped in PMMA, Journal of Physical Chemistry B 114 (2010) 13042–13051.

[10] P. Lenaerts, K. Driensen, R.V. Deun, K. Binnermans, Covalent coupling of luminescent tris(2-thenoyltrifluoroacetonato)lanthanide(III) complexes on a merrifield resin, Chemistry of Materials 17 (2005) 2148–2154.

[11] J. Kai, M.C.F.C. Felinto, L.A.O. Nunes, O.L. Malta, H.F. Brito, Intermolecular energy transfer and photostability of luminescence-tuneable multicolour PMMA films doped with lanthanide-β-diketonate complexes, Journal of Materials Chemistry 21 (2011) 3796–3802.

[12] Q.D. Ling, D.J. Liaw, C. Zhu, D.S.H. Chan, E.T. Kang, K.G. Neoh, Polymer electronic memories: materials, devices and mechanisms, Progress in Polymer Science 33 (2008) 917–978.

[13] V. Sankar, T.S. Kumar, K.P. Rao, Preparation, characterisation and fabrication of intraocular lens from photo initiated polymerised poly (methyl methacrylate), Trends in Biomaterials and Artificial Organs 17 (2004) 24–30.

[14] S. Jana, A.S. Khojin, W.H. Zhong, H. Chen, X. Liu, Q. Huo, Effects of gold nanoparticles and lithium hexafluorophosphate on the electrical conductivity of PMMA, Solid State Ionics 178 (2007) 1180–1186.

[15] S. Gross, D. Camozzo, V. Di Noto, L. Armelao, E. Tondello, PMMA: a key macromolecular component for dielectric low-κ hybrid inorganic–organic polymer films, European Polymer Journal 43 (2007) 673–696.

[16] K. Sheng, B. Yan, X.F. Qiao, L. Guo, Rare earth (Eu/Tb)/phthalic acid functionalized inorganic Si–O/organic polymeric hybrids: Chemically bonded fabrication and photophysical property, Journal of Photochemistry and Photobiology A: Chemistry 210 (2010) 36–43.

[17] H. Althues, R. Palkovits, A. Rumplecker, P. Simon, W. Sigle, M. Bredol, U. Kynast, S. Kaskel, Synthesis and characterization of transparent luminescent ZnS:Mn/PMMA nanocomposites, Chemistry of Materials 18 (2006) 1068–1072.

[18] S. Li, M.S. Toprak, Y.S. Jo, J. Dobson, D.K. Kim, Bulk synthesis of transparent and homogeneous polymeric hybrid materials with ZnO quantum dots and PMMA, Advanced Materials 19 (2007) 4347–4352.

[19] K. Rawlins, A. Lees, S. Fuerniss, K. Papathomas, Luminescence of $W(CO)_4$(4-Me-phen) in photosensitive thin films: a molecular probe of acrylate polymerization, Chemistry of Materials 8 (1996) 1540–1544.

[20] S.C. Farmer, T.E. Pattern, Photoluminescent polymer/quantum dot composite nanoparticles, Chemistry of Materials 13 (2001) 3920–3926.

[21] Z. Li, J. Zhang, J. Du, T. Mu, Z. Liu, J. Chen, B. Han, Preparation of cadmium sulfide/poly(methyl methacrylate) composites by precipitation with compressed CO_2, Journal of Applied Polymer Science 94 (2004) 1643–1648.

[22] A.V. Hayes, H.G. Drickamer, High pressure luminescence studies of energy transfer in rare earth chelates, Journal of Chemical Physics 76 (1982) 114–125.

[23] J. Gao, C. Lü, X. Lü, Y. Du, APhen-functionalized nanoparticles-polymer fluorescent nanocomposites *via* ligand exchange and *in situ* bulk polymerization, Journal of Materials Chemistry 17 (2007) 4591–4597.

[24] L. Chen, J. Zhu, Q. Li, S. Chen, Y. Wang, Controllable synthesis of functionalized CdS nanocrystals and CdS/PMMA nanocomposite hybrids, European Polymer Journal 43 (2007) 4593–4601.

[25] R. Palkovits, H. Althues, A. Rumplecker, B. Tesche, A. Dreier, U. Holle, G. Fink, C.H. Cheng, D.F. Shantz, S. Kaskel, Polymerization of w/o microemulsions for the preparation of transparent SiO_2/PMMA nanocomposites, Langmuir 21 (2005) 6048–6053.

[26] M. Avella, M.E. Errico, E. Martuscelli, Novel PMMA/$CaCO_3$ nanocomposites abrasion resistant prepared by an *in situ* polymerization process, Nano Letters 1 (2001) 213–217.

[27] Q. Xi, C. Zhao, J. Yuan, S. Cheng, The Effects of polymer-nanofiller interactions on the dynamical mechanical properties of PMMA/$CaCO_3$ composites prepared by microemulsion template, Journal of Applied Polymer Science 91 (2004) 2739–2749.

[28] S. Ahmad, S. Ahmad, S.A. Agnihotry, Synthesis and characterization of *in situ* prepared poly(methyl methacrylate) nanocomposites, Bulletin of Material Science 3 (2007) 31–35.

[29] J. Shen, X. Zheng, H. Ruan, L. Wu, J. Qiu, C. Gao, Synthesis of AgCl/PMMA hybrid membranes and their sorption performance of cyclohexane/cyclohexene, Journal of Membrane Science 304 (2007) 118–124.

[30] M. Avella, M.E. Errico, G. Gentile, PMMA based nanocomposites filled with modified $CaCO_3$ nanoparticles, Macromolecular Symposia 247 (2007) 140–146.

[31] R. Chai, H. Lian, P. Yang, Y. Fan, Z. Hou, X. Kang, J. Lin, *In situ* preparation and luminescent properties of $LaPO_4$:Ce^{3+}, Tb^{3+} nanoparticles and transparent $LaPO_4$:Ce^{3+}, Tb^{3+}/PMMA nanocomposite, Journal of Colloid and Interface Science 336 (2009) 46–50.

[32] C. Wang, J. Yan, X. Cui, D. Cong, H. Wang, Preparation and characterization of magnetic hollow PMMA nanospheres *via in situ* emulsion polymerization, Colloids and Surfaces A: Physicochemical and Engineering Aspects 363 (2010) 71–77.

[33] T.P. Mthethwa, M.J. Moloto, A. De Vries, K.P. Matabola, Properties of electrospun CdS and CdSe filled poly(methyl methacrylate) (PMMA) nanofibres, Materials Research Bulletin 46 (2011) 569–575.

[34] G.F. de Sá, O.L. Malta, C. de Mello Donegá, A.M. Simas, R.L. Longo, P.A. Santa-Cruz, E.F. da Silva Jr., Spectroscopic properties and design of highly luminescent lanthanide coordination complexes, Coordination Chemistry Reviews 196 (2000) 165–195.

[35] D.F. Parra, A. Mucciolo, H.F. Brito, L.C. Thompson, Optical characteristics of the Eu^{3+}-β-diketonate complex doped into epoxy resin, Journal of Solid State Chemistry 171 (2003) 412–419.

[36] M. Li, P.R. Selvin, Luminescent Polyaminocarboxylate chelates of terbium and europium: the effect of chelate structure, Journal of the American Chemical Society 117 (1995) 8132–8138.

[37] P.A. Santa-Cruz, F.S. Teles, Spectra Lux Software v.1.0, Ponto Quântico Nanodispositivos/RENAMI, 2003.